2
Engineering Enantioselectivity in Enzyme-Catalyzed Reactions

Romas Kazlauskas

2.1
Introduction

Enantioselective enzyme reactions are enzyme-catalyzed reactions that discriminate between enantiomeric substrates or products. For example, the kinetic resolution of a lactam is an enantioselective enzyme reaction (see Scheme 2.1). The lactamase catalyzes the hydrolysis of the (+)-lactam, leaving the unreacted (–)-lactam in high enantiomeric purity [1]. This (–)-lactam serves as the starting material for the synthesis of carbocyclic nucleosides such as abacavir. The enantioselectivity for this reaction is >400, which means that the (+)-lactam reacts more than 400 times faster than the (–)-enantiomer.

This chapter focuses on the use of protein engineering to increase enzyme enantioselectivity, and also provides a review of our current understanding of enantioselectivity and successes in protein engineering. The focus is on unnatural substrates such as the lactam shown in Scheme 2.1, because organic synthesis requires such reactions for the manufacture of pharmaceutical intermediates and fine chemicals. At this point, enantioselective inhibition, which is an important consideration in drug design because it involves only binding and not a chemical reaction, will not be considered.

Natural enzyme-catalyzed metabolic reactions may show very high selectivity because natural selection favors more efficient metabolic reactions. For example, L-lactate dehydrogenase from *Bacillus stearothermophilus* favors L-lactate over D-lactate by a ratio of more than 25 000 : 1 [2]. The evolutionary reason for this high enantioselectivity is probably not to discriminate against D-lactate, which is the end product of anaerobic metabolism where the formation of either enantiomer fulfills the biochemical role. The high enantioselectivity is most likely the byproduct of evolving a highly efficient catalyst for L-lactate. A catalyst perfectly fitted for L-lactate will be a poor fit for D-lactate.

As enzyme-catalyzed reactions involving unnatural substrates have not faced any evolutionary pressure, their enantioselectivities vary widely. Although the lactam example in Scheme 2.1 shows excellent enantioselectivity, many examples

Protein Engineering Handbook. Edited by Stefan Lutz and Uwe Theo

ISBN: 978-3-527-31850-6

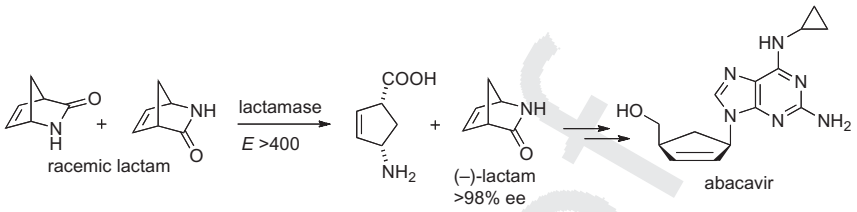

Scheme 2.1 Lactamase-catalyzed kinetic resolution of 2-azabicyclo(2.2.1)hept-5-en-3one (lactam) yields an enantiopure intermediate for synthesis of abacavir, an anti-AIDS drug.

demonstrate minimal enantioselectivity. For synthetic use, the enantioselectivity should be >50, although values as low as 20 may be synthetically useful if the product is very valuable and there are no alternative routes.

Enantioselective enzyme reactions can be either *kinetic resolutions* or *enantioselective syntheses*. Kinetic resolutions are separations (or partial separations) of enantiomers in a racemate due to a faster enzyme-catalyzed reaction for one of the two enantiomers. The lactamase example described above is a kinetic resolution. Because kinetic resolutions are separations, they produce a maximum of 50% yield of one enantiomer. The enantioselectivity in a kinetic resolution is the ratio of the specificity constants for the fast- and slow-reacting enantiomers (Equation 2.1). The measurement of all four kinetic constants is tedious, but the enantioselectivity can also be calculated from the measured enantiomeric purity of the products or starting materials at known extents of conversion [3]. The enantiomeric purity of the product decreases during a kinetic resolution because the starting material becomes enriched in the slow-reacting enantiomer as the reaction proceeds.

kinetic resolution:

$$E = (k_{cat}/K_m)_{\text{fast enantiomer}}/(k_{cat}/K_m)_{\text{slow enantiomer}} \tag{2.1}$$

Enantioselective syntheses start with a prochiral[1)] substrate and form predominantly one enantiomer of the product. Two examples of enantioselective syntheses (see Scheme 2.2) are a lipase-catalyzed hydrolysis of a diester to yield a chiral monoester [4, 5] and a dehydrogenase-catalyzed reduction of a prochiral ketone to yield a secondary alcohol [6]. Enantioselective syntheses can produce a 100% yield of one enantiomer. The disadvantage of enantioselective syntheses is the more limited range of starting materials as there are fewer prochiral molecules than racemates [7]. Chiral molecules typically have four different substituents, while prochiral molecules typically have only three different substituents. If n is the number of possible substituents, then there are n^4 chiral molecules, but only n^3 prochiral molecules.

1) A prochiral molecule is an achiral molecule which becomes chiral in a single desymmetrization step. The desymmetrization may be: (i) addition to one face of a double bond; or (ii) replacement or modification of one of two identical ligands.

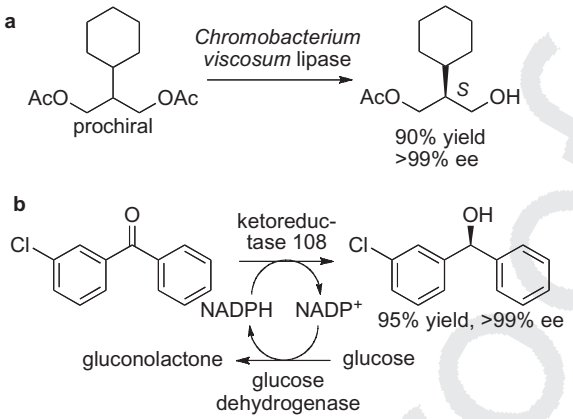

Scheme 2.2 Two examples of enzyme-catalyzed enantioselective syntheses. (a) A lipase-catalyzed hydrolysis of the prochiral diacetate favors hydrolysis to the (*S*)-monoacetate; (b) A dehydrogenase-catalyzed reduction of a diaryl ketone yields the (*S*)-diaryl secondary alcohol. The reduction of $NADP^+$ by glucose regenerates the NADPH.

For an enantioselective synthesis, the *enantioselectivity* is the ratio of the product enantiomers, which corresponds to their relative rates of formation (Equation 2.2). (The equation using enantiomeric excess (ee) is mathematically equivalent, but more convenient to use.) This ratio is constant in an enantioselective synthesis:

Asymmetric synthesis: E = amount of major product enantiomer/amount of minor product enantiomer or

$$E = (1 + \text{ee})/(1 - \text{ee}) \tag{2.2}$$

Another method of grouping enantioselective enzyme-catalyzed reactions is to group those that create a stereocenter, and those that only preserve an existing stereocenter. Reactions that create a stereocenter involve bond-making or bond-breaking at the stereocenter, whereas those that only preserve a stereocenter involve reactions adjacent to a stereocenter. The enantioselective reduction of a ketone to a secondary alcohol involves reaction at the stereocenter and falls into the first group, while the hydrolysis of an ester or lactam does not involve reaction at the stereocenter and falls into the second group. Reactions in the first group presumably require precise positioning of the stereocenter to allow reaction there, whereas those in the second group may tolerate a range of positions for the stereocenter. Many of the examples in the second group are kinetic resolutions, such as that in Scheme 2.1, but they can also include enantioselective syntheses such the desymmetrization of the diacetate in Scheme 2.2.

2.2
Molecular Basis for Enantioselectivity

2.2.1
Transition-State, Fast-Reacting Enantiomers Fit in the Active Site Better than Slow-Reacting Enantiomers

Enzymes are enantioselective because they stabilize the transition state for fast-reacting enantiomers more effectively than for slow-reacting enantiomers. Identification of the molecular basis for enantioselectivity requires the reacting orientations to be identified for both the fast- and slow-reacting enantiomers, as well as differences in their orientations. Orienting the fast-reacting enantiomer is usually straightforward; the reacting atoms are oriented to best interact with the catalytic machinery of the enzyme, while the remaining nonreacting substituents are placed to best fit any nearby pockets.

Orienting the slow-reacting enantiomer is less straightforward because different compromises are possible. For example, the slow enantiomer will clash with some features of an active site meant for the fast-reacting enantiomer. Moreover, different orientations will create different clashes, but may have similar energies. Typically, the slow enantiomer will react via the lowest energy orientations, although several orientations with low energy may contribute. The lowest energy orientations may differ for different substrates, and perhaps even for the same substrate under different conditions. Thus, any difficulties in identifying the molecular basis of enantioselectivity usually stem from problems in identifying the orientation of the slow-reacting enantiomer–that is, how the enzyme makes mistakes.

2.2.2
The Slow-Reacting Enantiomer Fits by Exchanging Two Substituents

One way to fit the slow enantiomer into a site matching the fast enantiomer is to exchange the location of two substituents. This exchange creates two mismatches between substituents and binding site. For example, *(S)*-2-hydroxyisocaproate dehydrogenase from *Lactobacillus confusus* shows high enantioselectivity toward α-hydroxycarboxylic acids [8]. The X-ray crystal structure [9] reveals an active site that could fit the substrate α-ketocarboxylic acid in two ways (Figure 2.1). In both cases, the catalytic groups are positioned for reaction: two hydrogen bonds to the carbonyl oxygen polarize the carbonyl group, and the hydride from nicotinamide is positioned for attack. The difference between the two orientations is the exchange between the R-group and the carboxylate, which leads to opposite enantiomers after the hydride transfer.

Two experimental results on reversing enantioselectivity support this proposed exchange of substituents. First, overlaying the X-ray structures of *(S)*-hydroxyisocaproate dehydrogenase and *(R)*-hydroxyisocaproate dehydrogenase from *Lactobacillus casei*, which favors the opposite enantiomer, shows that the two active sites differ by a reversed location for the hydrophobic pocket and the

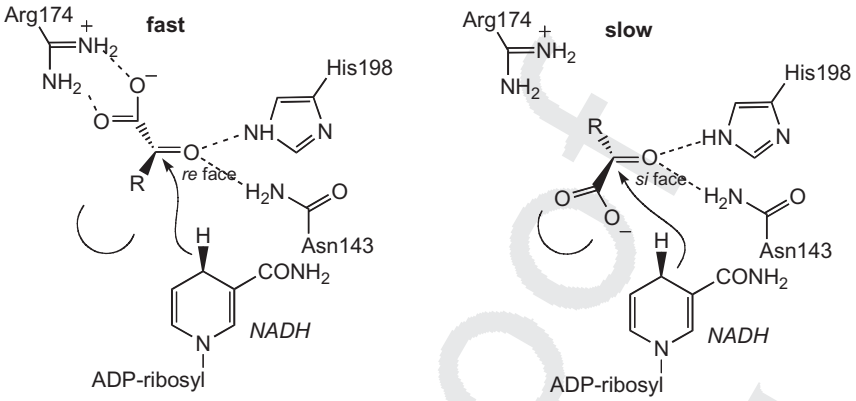

Figure 2.1 Schematic of an α-ketocarboxylic acid in the active site of *(S)*-hydroxyisocaproate dehydrogenase *Lactobacillus confusus* in two possible orientations, based on computer modeling of the substrate starting from the X-ray crystal structure (pdb code 1hyh). Addition of the hydride to the *re* face (left) yields the major *(S)*-alcohol, while addition to the *si* face (right) yields the minor *(R)*-alcohol. In both cases, the α-carbonyl oxygen is positioned by H-bonds from Asn143 and His198. The orientation of the two substituents differs. In the orientation leading to the major enantiomer, the carboxylate form hydrogen bonds to Arg174 and the hydrophobic R group sits in a hydrophobic pocket, represented by a semicircle. In contrast, the orientation leading to the minor enantiomer places the R group near Arg174 and the carboxylate in the hydrophobic pocket.

carboxylate-binding site [10] (see also Ref. [11]). Second, Jones and coworkers used site-directed mutagenesis to switch locations of the hydrophobic pocket and the carboxylate-binding site in a similar dehydrogenase, namely lactate dehydrogenase [2]. As expected, the enantioselectivity decreased but did not reverse, most likely because the mutagenesis did not completely switch the two sites. However, in several other cases described below, mutagenesis to exchange substituent sites did reverse the enantioselectivity.

Fitting the slow enantiomer into the active site by exchanging two substituents preserves the location of the stereocenter. This preservation is likely important for all reactions that involve bond breaking or bond making at the stereocenter. This exchange-of-substituents concept is the working hypothesis for most research groups investigating how enzymes 'make mistakes'. In order to increase enantioselectivity it is necessary to increase the ability of the enzyme to distinguish the substituents at the stereocenter; in the example above this is carboxylate and the hydrophobic R group in the dehydrogenase.

2.2.3
The Slow Enantiomer Fits by an Umbrella-Like Inversion

Despite this working hypothesis, the X-ray crystal structures of enantiomers bound to the active site of an enzyme usually do not show the exchange-of-two-

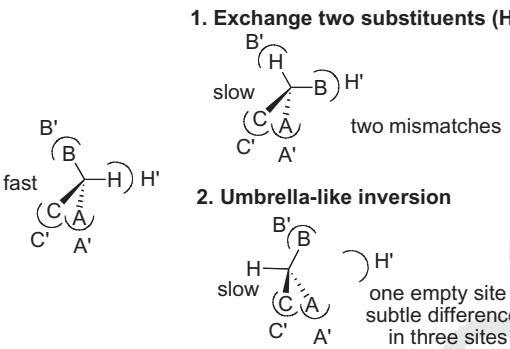

Figure 2.2 Two ways in which the slow enantiomer can fit into an active site that matches the fast-reacting enantiomer. For the fast enantiomer (left) all four interactions between the substituents (H, A, B, C) and the binding sites (H′, A′, B′, C′) match. To fit the slow enantiomer while preserving the location of the stereocenter (top right) requires exchanging two substituents, H and B in this example; there are five other possibilities. Only two substituents can match their binding sites. Another way to fit the slow enantiomer is via an umbrella-like inversion (bottom right) that leaves one site empty. This second possibility creates only one mismatch, but displaces the stereocenter slightly.

substituents orientation, but instead an umbrella-like inversion where only one substituent (usually hydrogen) lies in a new location [12]. (For details of earlier studies and an historical context, see Ref. [13].) One can imagine this orientation as follows. First, an inversion through the stereocenter creates the enantiomer by moving all four substituents to new locations. Second, a displacement moves three substituents into their previous locations, leaving one substituent (usually hydrogen) pointing in a new direction and the stereocenter slightly displaced from its original location (Figure 2.2). This umbrella-like-inversion orientation for the two enantiomers is most likely lower in energy because it creates only one mismatch between the substituents and the binding site, rather than two mismatches when the enantiomers adopt the exchange-of-substituents orientation.

This umbrella-like-inversion orientation may well be important only for reactions adjacent to the stereocenter, but not for those that make or break a bond at the stereocenter. The umbrella-like inversion shifts the position of the stereocenter, typically by 1 Å. This shift likely prevents catalysis when making or breaking a bond at the stereocenter (e.g. reduction of an α-ketocarboxylic acid, as above). However, when the reaction occurs adjacent to the stereocenter (hydrolysis of an ester of a secondary alcohol), then placement of the stereocenter is less critical and the umbrella-like inversion may be a catalytically productive orientation.

One example of X-ray structures showing such an umbrella-like-inversion are phosphonate transition-state analogues bound to the actives site of *Candida rugosa* lipase (CRL)[2)] [14] (Figure 2.3). The phosphonates mimic the transition states for

2) Microorganism names may change as investigators learn more about them. *Candida rugosa* is the same microorganism as *Candida cylindracea; Pseudomonas cepacia* is the same as *Burkholderia cepacia*.

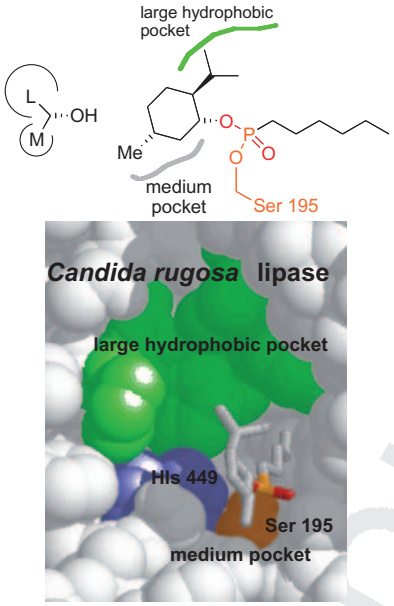

Figure 2.3 X-ray structure of the phosphonate transition-state analogue (sticks representation) for the hydrolysis of (1*R*)-menthyl heptanoate (fast-reacting enantiomer) in the active-site lipase from *Candida rugosa* (space-filling representation). Top: a generic structure of the fast-reacting enantiomer (L = large substituent; M = medium substituent) and a transition-state analogue for the fast-reacting enantiomer of menthol. Bottom: The active site contains a large and a medium pocket for the corresponding substituents in the substrate. The large substituent of the menthyl moiety (top half of cyclohexyl ring including the isopropyl substituent) binds in the large hydrophobic pocket (green), while the medium substituent (bottom part of the cyclohexyl ring including the methyl substituent) binds in the medium pocket. The catalytic residues are Ser 209 (orange) and His 449 (purple).

hydrolysis of the menthyl heptanoate esters. The CRL isoenzyme shown in the X-ray structure is highly enantioselective ($E > 100$) towards the *(1R)*-enantiomer of menthyl esters [15]. (Crude CRL is only moderately enantioselective ($E \sim 15$), most likely due to contaminating hydrolases with lower or reversed enantioselectivity.) The substituents at the alcohol stereocenter are: the alcohol oxygen; the isopropyl-substituted side of the cyclohexyl moiety (the large group, L); the unsubstituted side of the cyclohexyl moiety (the medium substituent, M); and hydrogen. The structures reveal an alcohol-binding site in the lipase that has one large and one medium pocket that match the relative sizes of the substituents.

A comparison of the X-ray crystal structure of transition-state analogues for the fast- and slow-reacting enantiomers of menthol bound to the active site of CRL shows an umbrella-like-inversion orientation (Figure 2.4). For both enantiomers, three substituents lie in similar locations: the large group remains in the large pocket, the alcohol oxygen lies near the phosphorus, and the medium substituent

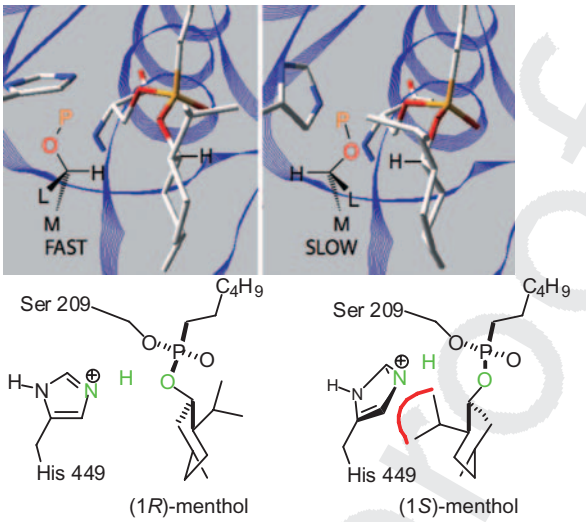

Figure 2.4 Comparison of transition-state analogues for the fast and slow enantiomers of menthol bound the active site of lipase from *Candida rugosa*. Top: X-ray structures reveal an umbrella-like-inversion orientation. The L, M and O substituents adopt similar locations, while the hydrogens lie in different locations. Bottom: The fast-reacting enantiomer of menthol (1*R*) shows the expected hydrogen bonds for catalysis. In contrast, the slow-reacting enantiomer lacks a key hydrogen bond, in part because the isopropyl substituent bumps the catalytic histidine. This lack of a hydrogen bond can account for the slower reaction.

lies in the medium pocket. The hydrogen locations differ as they point in opposite directions.

High enantioselectivity requires that CRL prevents all catalytically productive orientations of the slow-reacting enantiomer. For substituent-exchange, the most likely orientation is an exchange between the large and medium substituents, but the restricted size of the medium pocket likely prevents placement of the large substituent there. For the umbrella-like inversion orientation, the X-ray structures show a missing key hydrogen bond for the slow enantiomer. This bond cannot form for the slow enantiomer for two reasons. First, although the oxygen atom positions are similar, the oxygens are displaced by 0.7 Å. Second, the isopropyl group in the fast enantiomer lies to the right out of the way, while the isopropyl group in the slow enantiomer lies to the left and bumps the catalytic histidine, causing the imidazole ring to turn by ~60°. These two differences break a key hydrogen bond. Thus, by preventing reaction of the slow enantiomer via both substituent exchange and mirror image orientations, the lipase achieves high enantioselectivity.

Nonetheless, the slow enantiomer does react, albeit much more slowly than the fast enantiomer. Even in this well-studied example, it is not known how the slow enantiomer reacts. For example, it may crowd the large substituent into the

medium pocket, it may distort the orientation seen in the X-ray structure to restore the missing hydrogen bond, or it may use a water molecule bridge to restore the hydrogen bond. Several other possible orientations are discussed below. The exact pathway that the slow enantiomer takes to react most likely differs for different substrates and for different lipases.

The steady-state kinetics for enantioselective lipase-catalyzed resolutions fit either of the enantioselectivity mechanisms, and thus cannot distinguish between them. In most cases, the enantioselectivity stems primarily from differences in k_{cat}, the turnover number, with only small differences in the Michaelis constants, K_m. Examples include both chiral alcohols [16, 17] and chiral acids [18, 19]. This observation fits an umbrella-like inversion where both enantiomers bind similarly and thus with similar affinity, but subtle differences in the positioning of the substituents disrupt the catalysis. This observation also fits an exchange of substituents because K_m includes both the productive and nonproductive binding. Nonproductive binding lowers the value of k_{cat}; thus, if the fast enantiomer binds in a catalytically productive orientation, the slow enantiomer may bind similarly but cannot react in this orientation. The slow enantiomer then adopts a switched substituent orientation with poor binding via which it reacts. The measured kinetics will provide similar K_m values for both enantiomers and a lower k_{cat} for the slow enantiomer. There are, however, exceptions to this generalization, where enantioselectivity stems primarily from differences in K_m (for examples, see Refs [15, 17]). These differences in kinetic behavior suggest that there may be different enantioselectivity origins for different cases.

2.3
Qualitative Predictions of Enantioselectivity

2.3.1
Comparing Substrate Structures Leads to Empirical Rules and Box Models

Based on the observed enantioselectivity, various research groups have created generalizations that attempt both to summarize the observations and predict how a new substrate would behave. These generalizations were either generalized structures of substrates (e.g. a large or small substituent) or box models that suggested a shape for the active site [20]. Most of the models have focused on the size and shape of the substituents, most likely because a steric clash between atoms is the strongest intermolecular interaction. However, many of the models have also mentioned the polar or nonpolar character of substituents, indicating that size and shape is not the only feature that is important for high enantioselectivity.

One example of such a rule predicts which enantiomer of a secondary alcohol reacts fasters in lipase-catalyzed reactions (Figure 2.5). The rule is based on the size of the substituents, and applies to both hydrolysis and acylation reactions. For acylation, the enantiomer shown reacts faster, whereas for hydrolysis the ester of the enantiomer shown reacts faster.

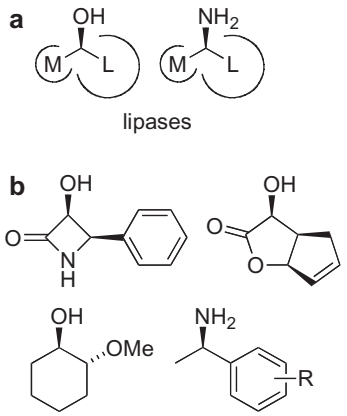

Figure 2.5 Empirical rules predict the fast-reacting enantiomer for lipases. Both secondary alcohols and amines of the type $RR'CHNH_2$ have similar structures, so similar rules apply. (a) Rules to predict the fast-reacting enantiomer for lipase-catalyzed reactions. M represents a medium-sized substituent such as methyl, while L represents a large substituent such as phenyl. In acylation reactions, the enantiomer shown reacts faster; in hydrolysis reactions, the ester of the enantiomer shown reacts faster; (b) Examples of pure enantiomers prepared by lipase-catalyzed reactions showing the fast-reacting enantiomer.

The advantage of this rule is that it is simple to apply. First, draw the substrate so that the alcohol (or ester) group points out of the page towards the reader. Second, imagine a line extending the C—O bond so that it divides the molecule into two parts. The enantiomer with the larger group on the right side of the line is the one that will react faster. Keep the flexibility of molecular structures in mind when comparing the sizes of the substituents. For instance, an alkyl chain can fold so that its effective size is smaller than a substituent which cannot fold, such as phenyl.

The rule for secondary alcohols applies to all lipases tested so far. These include cholesterol esterase (CE) [21], *Burkholderia cepacia* lipase (BCL) [2], lipases from several *Pseudomonas* species, including *Pseudomonas fluorescens* lipase (PFL) [22, 23], *Pseudomonas aeruginosa* lipase (PAL) [24], *Rhizomucor miehei* lipase (RML) [25], lipase B from *Candida antarctica* (CAL-B), and porcine pancreatic lipase [26]. The rule also works for CRL, but only for cyclic secondary alcohols [2], such as the menthol example discussed above.

This rule also applies to primary amines of the type $RR'CHNH_2$ because their shape is similar to that of secondary alcohols [27]. The lipases tested included CAL-B, BCL and PAL. Although lipases are very poor catalysts for the hydrolysis of amides, these lipases catalyze the reverse reaction, namely the acylation of amines.

2.3.2
Computer Modeling Based on X-Ray Structures of Enzymes

The X-ray structures of enzymes have revealed the extraordinary detail of the active site, and most current investigations utilize these structures or homology models to plan experiments. In many cases, computer modeling is used to rationalize behavior that could not be predicted by empirical rules because such rules lack detail or they apply only to certain classes of substrate.

For example, *Chromobacterium viscosum* lipase (CVL) catalyzes an enantioselective and regioselective kinetic resolution of a chiral bisphenol [28] (Figure 2.6). This phenol differs significantly from previously resolved molecules, so no empirical rule is available. Modeling shows that the alcohol-binding pocket of CVL tilts to one side, with the direction of this tilt matching the shape of the fast-reacting enantiomer. This modeling also shows that the butanoyl group best fits this tilt in the alcohol-binding pocket, which was consistent with the highest enantioselectivity for substrates with a butanoyl substituent. Smaller acyl groups would not fill the pocket, while larger groups would extend out of it. A similar rationalization based on modeling for chloroperoxidase (CPO) [29] shows how the shape of the active site favors the epoxidation of *cis*-1-phenyl-1-propene to the major 1*S*,2*R*-epoxide, and not to the minor 1*R*,2*S*-epoxide.

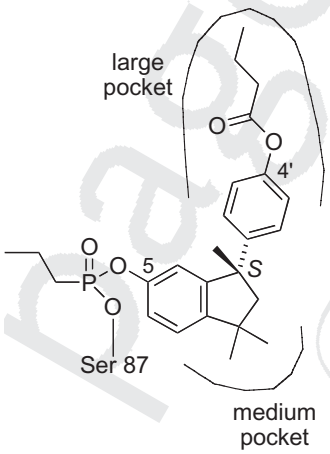

Figure 2.6 Line drawing of the phosphonate transition-state analogue for the CVL-catalyzed hydrolysis of favored butanoyl group: 5-position of the (*S*)-enantiomer. This regioisomer and enantiomer is favored by >30:1 over other possibilities. Energy minimization of the structure yielded the orientation shown. In the minimized structure for the other enantiomer the 4′-butanoyloxyphenyl group lies to the left, outside the large hydrophobic pocket. This difference in the orientation of the 4′-butanoyloxyphenyl group likely accounts for the faster reaction of the (*S*)-enantiomer.

Modeling has explained several puzzling observations about the resolution of carboxylic acids using CRL. Carboxylic acids with a stereocenter at the α-position orient the stereocenter near the mouth of a tunnel, with the large substituent inside the tunnel [30, 31]. Long-chain alcohols can also bind to the tunnel and compete with the favored enantiomer, thus lowering the enantioselectivity [12]. If the large substituent is extensively branched, then it no longer fits in the tunnel and the enantioselectivity reverses [32].

Modeling has also helped to explain how mutations can increase enantioselectivity. By using directed evolution, Reetz and coworkers discovered a lipase variant with a higher enantioselectivity towards 2-methyldecanoate esters. The wild-type was almost nonselective ($E = 1.1$), while the variant lipase with six amino acid substitutions showed an impressive increase to $E = 51$. Modeling suggested that one mutation – L162G – creates a pocket, while the other mutation – S53P – allows a nearby histidine side chain to stabilize the intermediate for the fast-reacting enantiomer. Modeling also suggested that the remaining four mutations either have no effect on enantioselectivity or even lower it. In agreement with this modeling, removing the other four mutations gave a double mutant with a slightly higher enantioselectivity ($E = 64$) than the variant from directed evolution [33, 34].

Although the relative energies of the modeled transition states for enantiomers rarely correspond to the measured enantioselectivities (see below), Pleiss and coworkers qualitatively correlated a calculated hydrogen bond distance with enantioselectivity [35]. BCL was shown to have a high enantioselectivity toward secondary alcohols. A comparison of models of the tetrahedral intermediate for enantiomeric secondary alcohols showed a long distance corresponding to an incomplete hydrogen bond for the slow enantiomer of well-resolved secondary alcohols ($E > 100$), but shorter distances corresponding to a catalytically productive hydrogen bond for moderately or poorly resolved secondary alcohols ($E < 20$).

2.3.3 What Is Missing from Current Computer Modeling?

Although computer modeling often provides a qualitative explanation of enantioselectivity, it remains very difficult to predict quantitatively the degree of enantioselectivity. This difficulty stems from the need to include a large number of conformations to create an accurate model; a single 'snapshot' cannot accurately describe a reaction.

One reason to include many conformations in a model is to include entropy. The activation energy for a chemical reaction is given by $\Delta G^{\ddagger}$. Enantioselectivity compares two reactions (those for each enantiomer), and is thus given by $\Delta\Delta G^{\ddagger}$. The latter term is related to the enantioselectivity, E, as $\Delta\Delta G^{\ddagger} = -RT\ln E$. This free energy difference consists of an enthalpic part, $\Delta\Delta H^{\ddagger}$ and a temperature-dependent entropic part, $\Delta\Delta S^{\ddagger}$:

$$\Delta\Delta G^{\ddagger} = -RT\ln S = \Delta\Delta H^{\ddagger} - T\Delta\Delta S^{\ddagger}$$

Although most investigators ignore the entropic term, assuming that it is small, experimental measurements (by measuring how enantioselectivity varies with temperature [36]) show that both entropy and enthalpy contribute similar amounts to enantioselectivity [37–40]. The entropic part is small only when both transition-state complexes for the enantiomers are equally rigid (both the substrate and enzyme side chains) and when the solvent interacts equally with both. Thus, modeling that omits entropy is unlikely to match experimental results.

Entropy calculations require additional steps beyond normal computer modeling, and are often combined with other modeling improvements. For example, Columbo *et al.* included both entropy calculations and a better assignment of partial charges in the transition state [21]. Their calculated enantioselectivity of $\Delta\Delta G^{\ddagger} = 1.25 \pm 0.5\,\text{kcal mol}^{-1}$ was close to the experimental value ($0.4\,\text{kcal mol}^{-1}$), but still inexact. These authors attributed the more accurate result mainly to partial charges, and not to the free energy calculation. Improved computational methods to calculate free energy continue to be an active area of research [41–43].

Another reason to include multiple conformation is to account for solvent effects. A solvent can change – and even reverse – the enantioselectivity of an enzyme (for examples, see Refs [44–46]). This change may be due to different solvation of the enantiomers by, for example, leaving different substituents exposed to a solvent. Enantiomers may also leave different parts of the active site exposed to solvent [47] or displace different numbers of solvent molecules from the active site [48]. Modeling normally uses approximations, such as continuum models, to account for solvent effects. Solvent water is usually treated as a distance-dependent dielectric – that is, the dielectric shielding increases with distance, mimicking solvation. Some computer modeling calculations include the individual water molecules found in the crystal structure, but not additional solvent water molecules. The most accurate (and most time-consuming) calculations surround the protein with individual solvent molecules and consider multiple orientations of solvent molecules.

Although quantum mechanics correctly describes electron configurations during reactions, these calculations are too complex for enzyme-catalyzed reactions. The alternative is molecular mechanics, where the calculations are fast but they rely on an approximate molecular description. Molecular mechanics treats molecules as balls attached to springs, where the force constants for the springs have been adjusted so they give the correct answer for known molecules. This physical picture of molecules is incorrect, as it is the delocalized molecular orbitals that hold the molecules together. The two solutions to this problem are: (i) the modeling of stable transition-state analogues with molecular mechanics; or (ii) a combination of quantum mechanics for the reactive portion and molecular mechanics for the rest of the model.

Phosphonates are an example of a stable transition-state analogue, as they mimic the transition state for ester hydrolysis and can be modeled using molecular mechanics. Although phosphonates [49] and other transition-state analogues only

approximate the true transition state, these approximations are minor compared to the other elements that are often missing from a computer model.

The modeling of a transition state directly requires a quantum mechanical description, and researchers combine quantum mechanics for the reactive region and molecular mechanics for the remainder of the protein in different ways. One approach is stepwise: here, quantum mechanics are used to model the transition state in the gas phase, after which the model is transferred to the enzyme and the calculation continued using molecular mechanics. A possible improvement is to calculate the transition state in the active site, using quantum mechanics. However, the distribution of partial charges changes significantly and the subsequent calculations more closely match the experimental results [50]. The most complex and accurate approach is to use simultaneous quantum mechanics for the active site region and molecular mechanics for the remainder of the protein [51]. These calculations also include the effects of the dynamic fluctuating electrostatic field from the protein and solvent.

Related to the problem of multiple conformations is the difficulty in finding the best conformations – that is, the conformations that have the lowest energies and catalytically productive orientations. The most common methods used are a systematic search (for a substrate with three or fewer rotatable bonds), the Monte Carlo method (which generates random conformations) and – most often – molecular dynamics (which creates a very short movie of molecular motion). Most problems are too large for a systematic search, while Monte Carlo methods are often inefficient because conformational change in enzyme complexes usually involves cooperative motion, which Monte Carlo methods model only poorly. Although molecular dynamics is the best way to search for alternate conformations of enzyme–transition-state complexes, it can also miss conformations. As the model mimics only a few nanoseconds of real time, any conformations that are separated from the starting conformation by a significant energy barrier, which requires infrequent motions to cross, may be missed.

As discussed above, the slow enantiomer may adopt an umbrella-like inversion orientation for reactions that do not involve bond making or bond breaking at the stereocenter, such as lipase-catalyzed reactions. In principle, a good conformational search will find these orientations, but in practice modeling has focused on the exchange of substituent orientations. Some research groups have suggested that BCL, CRL and CAL-B make mistakes via an M/L permutation [27, 52–54], while Nakamura *et al.* [55, 56] suggested that BCL makes mistakes via an M/H permutation (Figure 2.7). In the figure the X-ray structures of phosphonate transition-state analogues bound to CRL suggest that the umbrella-like inversion orientation is important. Clearly, if the conformation of the slow enantiomer is incorrect, then the predicted enantioselectivity will also be incorrect.

Although some of these proposals contradict each other, more than one may be correct. The orientation may differ for different lipases, or even for different secondary alcohols, with a single lipase. For example, it is reasonable that CRL with its large, open alcohol-binding site and CAL-B with its narrow, deep alcohol-binding site, might make mistakes by different pathways.

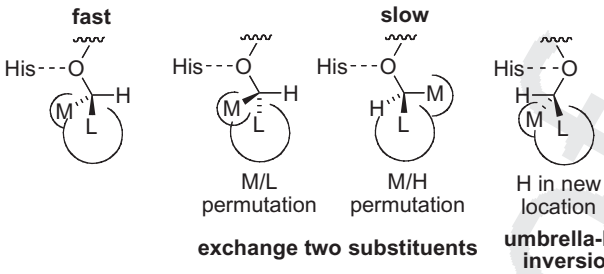

Figure 2.7 Possible orientations for the slow-reacting enantiomer of a secondary alcohol in the active site of lipase. The fast-reacting enantiomer orients with the large substituent into the page, the medium substituent into the page, and the hydrogen in the plane of the page. The slow enantiomer may fit into the same active site in several ways, while maintaining the key hydrogen bond between the oxygen and catalytic histidine. Accurate prediction of enantioselectivity requires knowing which orientations contribute to the reactivity of the slow enantiomer.

A more subtle problem in finding the global minimum occurs when two calculations yield the 'same' structure, but with slightly different energies. The energies differ because of small, presumably unimportant, differences far from the active site. For example, water molecules or side-chain orientation may differ on the surface of the enzyme. Minimization/molecular dynamics do not relax all such differences. One solution to this problem is careful model building; if the intention is to compare two structures, then one structure should be built and minimized, and then carefully modified to the other structure in a manner that does not introduce any unwanted differences. Hæffner *et al*. [57] suggested another solution to this problem. Instead of calculating the energies for the whole enzyme–transition-state complex, they calculated interaction energies only for the transition state and selected nearby residues. This approach eliminated presumably unimportant differences far from the active site and gave a closer agreement with measured enantioselectivities.

Finally, some reactions – electron or hydride transfer – may involve quantum mechanical tunneling, which is a new reaction path not included in classical transition state theory. The inclusion of quantum mechanic tunneling and the effects of protein motion on catalysis is an active area of research (e.g. see Ref. [58]), although others argue that that transition state theory can include all of these effects [59]. Monsan and coworkers have suggested that it is access to the active site, and not the transition state, which explains the enantioselectivity of a lipase towards 2-bromophenylacetic acids [60], although quantitative modeling of access also did not match the enantioselectivity.

2.4
Protein Engineering to Increase or Reverse Enantioselectivity

2.4.1
Mutations Closer to the Active Site Increase Enantioselectivity More Effectively than Mutations Far from the Active Site

Despite the incomplete understanding of enzyme enantioselectivity and the inability to quantitatively model enantioselective reactions, research groups have successfully engineered many dozens of enzyme variants with increased enantioselectivity. Some examples involve rational design, and others random mutagenesis and screening of the resultant variants. Although the molecular details differ in each case, it is possible to draw one simple generalization – that mutations closer to the active site lead to higher enantioselectivity increases than those far from the active site. This is not to say that distant mutations cannot increase enantioselectivity; there are some distant mutations that increase enantioselectivity, but the increases are smaller than the best examples lying closer to the active site. Furthermore, whilst not all close mutations increase enantioselectivity, the most effective mutations are found close to the active site.

These conclusions were derived from a survey of single amino acid substitutions in enzymes with known three-dimensional structure (Figure 2.8 and Table 2.1). The list includes both rational design and directed evolution experiments.

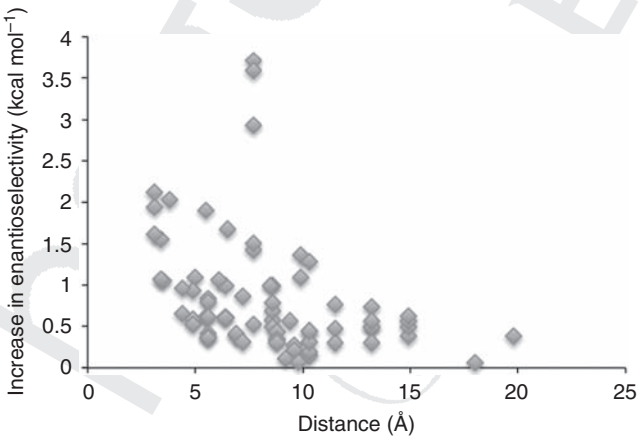

Figure 2.8 Location of single amino acid substitutions that increase enzyme enantioselectivity. The distances plotted along the x-axis are the distances from the stereocenter of the substrate to the closest nonhydrogen atom of the mutated amino acid. Enantioselectivity increases – expressed as activation free energy differences ($-\Delta\Delta G^{\ddagger}$) – lie along the y-axis. The biggest increases in enantioselectivity occur when the substitutions are close to the substrate.

The increases in enantioselectivity from wild-type to variant are given as free energies using $-\Delta\Delta\Delta G^{\ddagger} = RT\ln(E_{\text{mutant}}/E_{\text{wild-type}})$. The distances are from the key active site residue (or the stereocenter of the substrate) and closest nonhydrogen atom of the original amino acid. These distances are an upper limit as the substrate extends beyond the stereocenter or key active site residue. In addition, induced-fit or enzyme motion may move them toward one another. Distances of 5–8 Å indicate that the mutated amino acid probably contacts the substrate directly.

The enzymes in which the mutations caused the largest increase in enantioselectivity were a phosphotriesterase, horseradish peroxidase and a lipase [49, 52, 63]. For the phosphotriesterase, the most successful single mutation was Gly60Ala (amino acid residue at position 60 changed from glycine to alanine), which increased the enantioselectivity from 21 to 11 000 (520-fold, $-\Delta\Delta\Delta G^{\ddagger} = 3.7\,\text{kcal mol}^{-1}$) for the hydrolysis of *p*-nitrophenyl ethyl phenyl phosphate [63] (Figure 2.9). This mutation was chosen rationally from the crystal structure with a bound substrate analogue to decrease the size of the small binding pocket of the active site. Although, the phosphorus stereocenter of a bound inhibitor lies 7.7 Å from the Gly60, this overestimates the interaction distance. The isopropyl group of the inhibitor lies only 4.3 Å away, and the methyl side chain in the Ala variant will lie even closer. For horseradish peroxidase, a Phe41Leu mutation, also chosen by rational design, increased enantioselectivity up to 35-fold ($-\Delta\Delta\Delta G^{\ddagger} = 2.1\,\text{kcal mol}^{-1}$) for the sulfoxidation of thioethers [49]. This mutation was also chosen rationally, based on structures of related peroxidases to increase the accessibility of the substrate to the active site. The crystal structure of horseradish peroxidase has since been solved and shows that Phe41 is 3.1 Å from the hydroxamate oxygen of a bound inhibitor. For PAL, the best mutation was Leu162Gly, identified through directed evolution. This single mutation increased the enantioselectivity from 1.1 to 34 ($-\Delta\Delta\Delta G^{\ddagger} = 2.0\,\text{kcal mol}^{-1}$) towards *p*-nitrophenyl 2-methyldecanoate [52]. This amino acid residue was only 3.8 Å from the stereocenter of the substrate.

This survey also shows that distant mutations (>10 Å from the substrate) can improve enantioselectivity (19 of 71 examples in Table 2.1), albeit less effectively. The molecular mechanism for these changes may be a propagation of structural changes to the active site where they cause subtle structural changes. A chemical example of such a 'domino effect' showed that a series of conformational changes in amides controlled the stereochemistry of a bond 25 Å away [86]. A few of the 'distant' mutations may be an artifact of the distance definition. As mentioned above for horseradish peroxidase, the distance between substrate substituents and amino acid side chains is likely shorter than the distance to the substrate stereocenter. The distance also shortens when the introduced amino acid is larger than the original one. However, the amount of data available differs for each experiment and this imperfect definition of distance allows inclusion of a wide range of experiments.

Several other lines of evidence also suggest that closer mutations are more effective than distant ones in increasing enantioselectivity. First, the proportion of

Table 2.1 Single mutations that increase enantioselectivity and the distance of these mutations from the active site.[a]

Enzyme	Mutation	ΔE	Distance (Å)	$\Delta\Delta\Delta G^{\ddagger}$ (kcal mol^{-1})	Reference(s)
Horseradish peroxidase	F41L	5.5 to 199 (2-naphthalenyl methylsulfide), 1.2 to 32 (phenyl cyclopropylsulfide), 2.1 to 32 (phenyl ethylsulfide)	3.1[b]	2.12, 1.94, 1.61	[61, 62]
Agrobacterium radiobacter AD1 epoxide hydrolase	F108I	3.4 to 20 (*p*-nitrophenyl glycidyl ether)	3.5[c]	1.05	[63]
Candida antarctica lipase B	T40V, A	1.6 to 22, 9.8 (ethyl 2-hydroxypropanoate)	3.4	1.55, 1.07	[64]
Pseudomonas aeruginosa lipase	L162G	1.1 to 34 (*p*-nitrophenyl 2-methyldecanoate)	3.8	2.03	[65]
Pseudomonas fluorescens esterase	V121S, M	12 to 61, 36 (methyl 3-bromo-2-methylpropanoate)	4.4	0.96. 0.65	[53]
Pseudomonas fluorescens esterase	W28L, F, Y	12 to 58, 32, 29 (methyl 3-bromo-2-methylpropanoate)	4.9	0.93, 0.58, 0.52	[66]
Bacillus subtilis p-nitrobenzyl esterase	G105A	3 to 19 (2-phenyl-3-butin-2-yl acetate)	5[d]	1.09	[67]
Burkholderia cepacia lipase	I287F, A287F	44 to 123, 5 to 123 (2-cyclohexyl ethanol)	5.5[e]	0.61, 1.90	[68]
Agrobacterium radiobacter AD1 epoxide hydrolase	Y215F	100 to 200 (*p*-nitrostyrene oxide), 16 to 30 (styrene oxide), 6.5 to 12 (m-chlorostyrene oxide), 32 to 130 (*p*-chlorostyrene oxide)	5.6[c]	0.41, 0.37, 0.36, 0.83	[69]

Agrobacterium radiobacter AD1 epoxide hydrolase	Y215H	3.4 to 13 (*p*-nitrophenyl glycidyl ether), 56 to 156 (*p*-nitrostyrene oxide)	5.6[c]	0.79, 0.61	[50]
Agrobacterium radiobacter AD1 halohydrin dehalogenase	W249F	150 to 900 (*p*-nitro-2-brom-1-phenylethanol)	6.1	1.06	[70]
Rhizopus oryzae lipase	L258F	5 to 14 (1,3-dioleoyl-2-deoxy-2-palmitoylaminolglycerol), 8 to 22 (1,3-dioleoyl-2-deoxy-2-phenylglycerol)	6.4	0.61, 0.6	[71]
Salmonella enterica acid phosphatase	N151D	3.4 to 18.1 (*O*-phosphoserine)	6.4[f]	0.99	[72]
Escherichia coli penicillin G acylase	F24A	48 to 810 (glutamine)	6.5	1.67	[73]
Candida antarctica lipase B	S47A	6.5 to 12.5 (1-bromo-2-octanol), 14 to 28 (1-chloro-2-octanol)	6.9	0.39, 0.41	[74]
Arthrobacter sp. DSM 9771 hydantoinase	I95F, L	0.4 to 1.6 (L-5-(2-methylthioethyl)hydantoin)	7.2[g]	0.86, 0.31	[75]
Pseudomonas diminuta phosphotriesterase	G60A	1 to 11 (methyl ethyl *p*-nitrophenylphosphate), 32 to 400 (methyl isopropyl *p*-nitrophenylphosphate), 93 to 13 000 (methyl phenyl *p*-nitrophenylphosphate), 10 to 24 (ethyl isopropyl *p*-nitrophenylphosphate), 21 to 11 000 (ethyl phenyl *p*-nitrophenylphosphate), 35 to 15 000 (isopropyl phenyl *p*-nitrophenylphosphate)	7.7	1.42, 1.5, 2.93, 0.52, 3.71, 3.59	[76, 77]
Agrobacterium radiobacter AD1 epoxide hydrolase	I219F	17 to 91 (styrene oxide)	8.5[c]	0.99	[78]

Table 2.1 *Continued*

Enzyme	Mutation	ΔE	Distance (Å)	$\Delta\Delta\Delta G^{\ddagger}$ (kcal mol^{-1})	Reference(s)
Pseudomonas putida benzoylformate decarboxylase	L476 H, A, P, S, M, G Q, C, K	12 to 28–66 (2-hydroxy-1-phenylpropanone)	8.6[h]	0.49, 0.78, 0.57, 0.57, 0.57, 0.57, 0.68, 0.68, 0.99	[79]
Aspergillus niger M200 epoxide hydrolase	A217C, Q, L	2.4 to 5.0 (benzyl glycidyl ether)	8.8[i]	0.43, 0.34, 0.30	[80]
Salmonella enterica acid phosphatase	V78L	3.4 to 4.1 (*O*-phosphoserine)	9.2[f]	0.11	[59]
Pseudomonas aeruginosa lipase	S53P	1.2 to 3.1 (*p*-nitrophenyl 2-methyldecanoate)	9.4	0.56	[30]
Pseudomonas fluorescens esterase	T230I, P	12 to 19 (methyl 3-bromo-2-methylpropanoate)	9.6	0.27, 0.21	[69]
Pseudomonas aeruginosa lipase	L110R	10.7 to 12 (p-nitrophenyl 2-methyldecanoate)	9.8[j]	0.07	[30]
Arthrobacter sp. DSM 9771 hydantoinase	V154A	2.7 to 28 (5-(2-methylthioethyl)hydantoin)	9.9[c]	1.36	[62]
Alicyclobacillus acidocaldarius esterase	L212P	1.2 to 6.6 (*p*-nitrophenyl 2-chloropropanoate)	9.9	1.09	[81]
Pseudomonas aeruginosa lipase	S155F	Varies with generation due to other mutations (*p*-nitrophenyl 2-methyldecanoate)	10.3	0.15, 0.19, 0.31, 0.44	[30]
Pseudomonas aeruginosa lipase	S155L	1.1 to 4.4 (*p*-nitrophenyl 2-methyldecanoate)	10.3	0.44	[33]
Pseudomonas aeruginosa lipase	V47G	4.4 to 9.7–20.5 (*p*-nitrophenyl 2-methyldecanoate)	11.5	0.47, 0.76	[30]

Thermomyces lanuginosa lipase	E87A	10.5 to 17.4 (heptyl 2-methyldecanoate)	11.5[k]	0.3	[82]
Pseudomonas fluorescens esterase	D158N, E, L, C, F	3.5 to 5.8–12 (ethyl 3-phenylbutyrate)	13.2	0.3, 0.49, 0.73, 0.49, 0.56	[69]
Pseudomonas fluorescens esterase	L181Q, W, T, S	3.5 to 6.6–10 (ethyl 3-phenylbutyrate)	14.9	0.38, 0.49, 0.56, 0.62	[83]
Pseudomonas aeruginosa lipase	F259L	9.7 to 10.7 (*p*-nitrophenyl 2-methyldecanoate)	18.0	0.06	[30]
Pseudomonas aeruginosa lipase	S149G	1.1 to 2.1 (*p*-nitrophenyl 2-methyldecanoate)	19.8	0.38	[30]

a Criteria: Only increases in enantioselectivity caused by single mutations where the structure of the enzyme, or a very similar one, is known. Free energy values are calculated at 298 K. Distances are from the stereocenter of the substrate to closest nonhydrogen atom of the amino acid to be changed. Note that this definition of distance differs from that in Ref. [84], which used the distance to the Cα atom of the changed amino acid. The current definition usually gives shorter distances that the previous definition, but still overestimates the interaction distance in many cases.
b Distance is to the hydroxamate oxygen of a bound inhibitor in protein data bank file 2atj.
c No model containing substrate was available; distance to closest Oδ of active site Asp107.
d No model containing substrate was available; distance to Oγ of active site Ser189.
e Based on the crystal structure of a related *Burkholderia cepacia* lipase protein data bank file 1ys1, which has a leucine at position 287, not isoleucine. The side chain of isoleucine may be closer to the stereocenter. The A287F mutation refers to starting with the I287A variant, which has a lower enantioselectivity than the wild-type.
f Distance to Nε2 of His197 based on a homology model built by SwissModel [85] using an X-ray crystal structure of an acid phosphatase that has 96% sequence identity: protein data bank file 2ipd.
g Distance to active site Zn1.
h Distance to the closest atom (carboxylate oxygen) of a bound inhibitor, (*R*)-mandelate: protein data bank file 1mcz.
i Distance to closest Oδ of the active site aspartate based on a homology model built by SwissModel [71] using an X-ray crystal structure of an epoxide hydrolase that has 87% sequence identity: protein data bank file 1qo7.
j Residue 110 in protein data bank file 1ex9 is Lys not Leu; however this is the distance to Leu 118.
k The X-ray structure contained an oleic acid bound in a catalytically nonproductive orientation. The distance is from the amide nitrogen of Glu87 and C9 of the oleic acid, which lies approximately where a 2-stereocenter would lie in a productive orientation.

variants with increased enantioselectivity was higher when the changes were close to the active site. Mutations of the entire *Pseudomonas fluorescens* esterase (PFE) using error-prone PCR yielded <1% of catalytically active variants with increased enantioselectivity. These mutations were far (13–15 Å) from the substrate-binding site [69]. In contrast, focusing the mutations into the substrate-binding site using saturation mutagenesis yield 13% improved variants. There were a total of 76 possible mutants, of which approximately half were catalytically active. Five of these (13%) showed increased enantioselectivity and the increases in enantioselectivity were much higher (up to fivefold to $E = 61$) [53]. Another line of evidence is that computations and experiments with organometallic catalysts show that stereodirecting groups close to the reaction center give higher enantioselectivity than distant ones [87]. Organometallic catalysts and enzymes use the same physical principles to distinguish enantiomers, so these conclusions most likely also apply to enzymes. Lastly, the hypervariable region of antibodies lies in the antigen-binding site, which also suggests that closer mutations are the best way to change the binding specificity. As antibodies do not normally catalyze reactions this example might not apply to enzymes.

2.4.2 Reversing Enantioselectivity by Exchanging Locations of Binding Sites or a Catalytic Group

In approximately a dozen cases, research groups have achieved a more challenging goal, namely to reverse the enantioselectivity of an enzyme using protein engineering (Table 2.2) [10]. This reversal usually involves multiple amino acid substitutions, the most likely molecular basis for the reversal being either exchanged locations for two substituents or a switch in the location of a catalytic residue. Table 2.2 includes only examples where the enantioselectivity for both wild-type and variant is >5, and so omits partial successes where protein engineering mainly destroyed the enantioselectivity.

One example of exchanging locations for two substituents is the engineered reversal of enantioselectivity of organophosphorus hydrolase (OPH) (see Figure 2.9). OPH shows moderate enantioselectivity ($E = 21$) toward phosphate triesters such as *p*-nitrophenyl ethyl phenyl phosphate [63]. The hydrolysis favors the S_P enantiomer of the substrate but yields an achiral product, a phosphorus diester. The substrate-binding pocket contains a small and a large subsite. As mentioned above, decreasing the size of the small subsite by making a Gly60Ala mutation increases the enantioselectivity from $E = 21$ to >100. In order to reverse the enantiopreference, Raushel and coworkers first increased the size of the small subsite with three amino acid substitutions, which eliminated the enantioselectivity. Next, they decreased the size of the large subsite with a histidine to tyrosine substitution to increase the enantioselectivity to >100, favoring the R_P enantiomer. A similar mutant showed a reversed enantiopreference to methyl phenyl phosphinate esters [97].

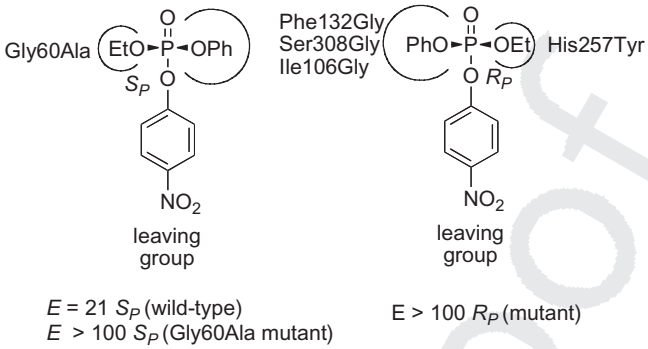

Figure 2.9 Organophosphorus hydrolase catalyzes the enantioselective hydrolysis of phosphate triesters. The wild-type enzyme favors the S_P enantiomer of *p*-nitrophenyl ethyl phenyl phosphate ($E = 21$). Decreasing the site of the small site using a Gly60Ala mutation increased enantioselectivity to $E > 100$. Reversing the relative sizes of the subsites using the four mutations shown reverses the enantiopreference.

Such pairwise mutagenesis in the active site may be the best strategy for reversing enantiopreference because reversal involves cooperativity, switching the location of not a single substituent but two substituents of the chiral substrate. Indeed, multiple mutations have reversed the enantioselectivity of horseradish peroxidase, BCL (two examples) and esterase from *Burkholderia gladioli*. Of the 11 examples listed in Table 2.2, only two used a single mutation: a Phe352Val mutation in the active site of naphthalene dioxygenase, which reversed its enantiopreference in the hydroxylation of biphenyl [32]; and the Trp104Ala mutation in the active site of CAL-B, which reversed its enantiopreference in the acylation of 1-phenylethanol. In both cases, enantioselectivity was decreased from high ($E > 100$) to moderate towards the other enantiomer (7.7 and 6.6, respectively). This suggested that additional mutations on the other side of the active site might increase enantioselectivity towards the newly preferred enantiomer. Changing the reaction solvent can also reverse the enantioselectivity [35], most likely due to solvation changes in the solvent-exposed portions of the substrate. However, this approach affects only the solvent-exposed substituent and has been less effective than protein engineering.

Although directed evolution has also reversed the enantioselectivity of enzymes, it required multiple mutations, possibly due to the difficulty of discovering cooperative mutations. Reetz and coworkers dramatically reversed the enantiopreference for PAL [64]. The wild-type lipase was nonselective towards 2-methyldecanoate esters ($E = 1.1$), but repeated random mutagenesis with different strategies, combined with screening, yielded two variants with good selectivity for opposite enantiomers. The *(R)*-selective lipase ($E = 30$) differed from the wild-type by 11 amino acid substitutions, while the *(S)*-selective lipase ($E = 51$) differed in

Table 2.2 Reversing the enantioselectivity by protein engineering.

	Substrate	Product	Mutation(s)	Enantioselectivity Reversal	Reference
Organophosphorus hydrolase	Ethyl phenyl 4-nitrophenyl phosphate	Ethyl phenyl diphosphate (achiral)	His257Tyr Phe132Gly Ser308Gly Ile106Gly	$E = 21$ (S_P)[a] to $E > 100$ (R_P)	[63]
Naphthalene dioxygenase	Biphenyl (achiral)	*cis*-3,4-dihydroxy-3,4-dihydrobiphenyl	Phe352Val	$E > 100$ (3*R*, 4*S*) to $E = 7.7$ (3*S*, 4*R*)	[88]
Horseradish peroxidase	Thioanisole	Methyl phenyl sulfoxide	Leu41His His42Ala	$E = 66$ (S)[b] to $E > 100$ (R)	[49]
Lipase from *Burkholderia cepacia*	1,4-Dihydropyridine diester	1,4-Dihydropyridine monoester carboxylic acid	Phe221Leu Val266Leu Leu287Ile	$E = 6.5$ (R) to $E > 100$ (S)	[89]
Lipase from *Burkholderia cepacia*	Ethyl 3-phenylbutyrate	3-Phenylbutyrate	Leu17Phe[c] Phe119Leu Leu167Gly Leu266Val	$E = 33$ (S) to $E = 38$ (R)	[90]

Esterase from *Burkholderia gladioli*	Methyl 2-hydroxy-2-methylpropanoate	2-Hydroxy-2-methylpropanoic acid	Leu135Phe Ile152Asn Val351Ser His253Phe	$E = 6.1$ (S) to $E = 29$ (R)	[91]
Esterase from *Bacillus subtilis*	1,1,1-Trifluoro-2-phenylbut-3-yn-1-yl acetate	1,1,1-Trifluoro-2-phenylbut-3-yn-1-ol	Asp188Trp Met193Cys[d]	$E > 100$ (R) to $E = 64$ (S)	[92]
Lipase from *Pseudomonas aeruginosa*	*p*-Nitrophenyl 2-methyldecanoate	2-Methyldecanoate	*Seventeen substitutions*[e]	$E = 51$ (S) to $E = 30$ (R)	[93]
Lipase B from *Candida antarctica*	1-Phenylethanol	1-Phenylethyl butyrate	Trp104Ala	E 200 (R) to $E = 13$ (S)	[94]
Vanillyl-alcohol oxidase	4-Ethylphenol (achiral)	4-(1′-hydroxyethyl)phenol	Asp170Ser Thr457Glu	$E = 32$ (R) to $E = 9$ (S)	[95]
Aryl malonate decarboxylase	α-Methyl-α-(2-thienyl)malonic acid	α-(2-thienyl)propionic acid	Gly74Cys Cys188Ser	$E > 100$ (S) to $E = 32$ (R)	[96]

a Raushel and coworkers could also increase the S_P-selectivity of the wild-type enzyme to >100 with a Gly60Ala mutation, which decreased the size of the small subsite.
b The (S)-selective enzyme is the Phe41Leu mutant. Wild-type horseradish peroxidase shows a lower enantioselectivity of $E = 6$.
c Both variants with reversed enantioselectivity contained the four mutations listed. In addition, one contained a Thr251Ala mutation, while the other contained an Asp21Asn mutation. The authors suggest that these additional mutations have little effect on enantioselectivity.
d The wild-type is Glu188 not Asp188, but the Asp188 variant shows higher enantioselectivity.
e The wild-type enzyme showed almost no enantioselectivity ($E = 1.1$). The (R)-selective mutant contained 11 amino acid substitutions as compared to wild-type, while the (S)-selective enzyme contained a different set of six amino acid substitutions compared to wild-type. None of the mutations involved active site residues.

six other substitutions. Thus, the reversal in this case requires 17 amino acid substitutions.

The last two entries in Table 2.2 repositioned catalytic groups to reverse enantiopreference. Vanillyl-alcohol oxidase (VAO) catalyzes the enantioselective oxidation of 4-ethylphenol to *(R)*-1-(4′-hydroxyphenyl)ethanol ($E = 32$), while the structurally related *p*-cresol methylhydroxylase (PCMH) forms the *(S)*-enantiomer ($E \sim 2$). The oxidation involves oxidation of the phenol to the quinone methide intermediate by the flavin cofactor, followed by the addition of water to one face of the quinone methide to form the product alcohol. The X-ray structures revealed an aspartate residue in VAO near one face of the intermediate, and a glutamate residue in PCMH near the opposite face. It was hypothesized that these catalytically equivalent carboxylate groups positioned a water molecule to form the *(R)*-alcohol in VAO and the *(S)*-alcohol in PCMH. Van den Heuvel and coworkers tested this hypothesis by reversing the enantiopreference of VAO. They prepared a double mutant of VAO, Asp170Ser/Thr457Glu, which removed the aspartate from one side of the intermediate and introduced a glutamate on the other side. As predicted, this double mutant showed opposite enantioselectivity and formed *(S)*-1-(4′-hydroxyphenyl)ethanol ($E = 9$).

In another example, Ohta and coworkers reversed the enantiopreference of an arylmalonate decarboxylase by moving the cysteine residue to the other side of the active site.

2.5 Concluding Remarks

The enantioselectivity of enzyme-catalyzed reactions will continue to be important because it raises fundamental scientific questions, and because of the practical importance of pure enantiomers to the pharmaceutical industry. Enantioselectivity is a fundamental property of biological systems; indeed, pure enantiomers are all derived from biosynthesis either directly as natural products or as products of enzyme-catalyzed syntheses or indirectly via chemical synthesis using auxiliaries derived from biosynthesis. A rare exception to this statement is the direct crystallization of enantiomers, similar to the first resolution of tartrate salts by Pasteur, which uses the crystal lattice for enantiomer recognition.

Enantioselectivity is also an excellent place to test our understanding of molecular recognition because enantiomers have identical physical and chemical properties, and differ only in their shape. In contrast, selectivity between different molecules or diastereomers can be complicated by solubility differences, conformer distribution differences, and even reactivity differences.

Protein engineering can improve and even reverse the enantioselectivity of enzymes. Currently, the approach is qualitative and still relies on the chemical insights of the researcher as well as a little luck. Reliable predictions will require not only the quantitative prediction of enantioselectivity, as discussed above, but

also a prediction of protein folding, reactivity and stability so that the variant produced is a good and stable catalyst.

References

1 Taylor, S.J.C., Holt, K.E., Brown, R.C., Keene, P.A. and Taylor, I.N. (2000) Choice of biocatalyst in the development of industrial biotransformations, in *Stereoselective Biocatalysis* (ed. R.M. Pateland), Marcel Dekker, New York, pp. 397–413.

2 Sakowicz, R., Gold, M. and Jones, J.B. (1995) Partial reversal of the substrate stereospecificity of an L-lactate dehydrogenase by site-directed mutagenesis. *Journal of The American Chemical Society*, **117**, 2387–94.

3 Chen, C.S., Fujimoto, Y., Girdaukas, G. and Sih, C.J. (1982) Quantitative analyses of biochemical kinetic resolutions of enantiomers. *Journal of the American Chemical Society*, **104**, 7294–9.

4 Patel, R.N., Robison, R.S. and Szarka, L.J. (1990) Stereoselective enzymic hydrolysis of 2-cyclohexyl- and 2-phenyl-1,3-propanediol diacetate in biphasic systems. *Applied Microbiology and Biotechnology*, **34**, 10–14.

5 Patel, R.N. (2000) Stereoselective biocatalysis for synthesis of some chiral pharmaceutical intermediates, in *Stereoselective Biocatalysis* (ed. R.M. Patel), Marcel Dekker, New York, pp. 87–130.

6 Truppo, M.D., Pollard, D. and Devine, P. (2007) Enzyme-catalyzed enantioselective diaryl ketone reductions. *Organic Letters*, **9**, 335–8.

7 Gruber, C.C., Lavandera, I., Faber, F. and Kroutil, W. (2006) From a racemate to a single enantiomer: deracemization by stereoinversion. *Advanced Synthesis Catalysis*, **348**, 1789–805.

8 Schütte, H., Hummel, W. and Kula, M.-R. (1984) L-2-Hydroxyisocaproate dehydrogenase–a new enzyme from *Lactobacillus confusus* for the stereospecific reduction of 2-ketocarboxylic acids. *Applied Microbiology and Biotechnology*, **19**, 167–76.

9 Niefind, K., Hecht, H.J. and Schomburg, D. (1995) Crystal structure of L-2-hydroxyisocaproate dehydrogenase from *Lactobacillus confusus* at 2.2 A resolution. An example of strong asymmetry between subunits. *Journal of Molecular Biology*, **251**, 256–81.

10 Dengler, U., Niefind, K., Kiess, M. and Schomburg, D. (1997) Crystal structure of a ternary complex of D-2-hydroxyisocaproate dehydrogenase from *Lactobacillus casei*, NAD^+ and 2-oxoisocaproate at 1.9 Å resolution. *Journal of Molecular Biology*, **267**, 640–60.

11 Mugford, P.F., Wagner, U., Jiang, Y., Kurt Faber, K. and Kazlauskas, R.J. (2008) Enantiocomplementary enzymes: classification, molecular basis for their reversed enantiopreference and prospects for mirror-image biotransformations. *Angewandte Chemie–International Edition*, **47**, ••–••.

12 Mezzetti, A., Schrag, J.D., Cheong, C.S. and Kazlauskas, R.J. (2005) Mirror-image packing in enantiomer discrimination: molecular basis for the enantioselectivity of *B. cepacia* lipase toward 2-methyl-3-phenyl-1-propanol. *Chemistry and Biology*, **12**, 427–37.

13 Bentley, R. (2003) Diastereoisomerism, contact points, and chiral selectivity: a four-site saga. *Archives of Biochemistry and Biophysics*, **414**, 1–12.

14 Cygler, M., Grochulski, P., Kazlauskas, R.J., Schrag, J.D., Bouthillier, F., Rubin, B., Serreqi, A.N. and Gupta, A.K. (1994) Molecular basis for the chiral preference of lipases. *Journal of the American Chemical Society*, **116**, 3180–6.

15 Vorlova, S., Bornscheuer, U.T., Gatfield, I., Hilmer, J.M., Bertram, H.J. and Schmid, R.D. (2002) Enantioselective hydrolysis of D,L-menthyl benzoate to L-(–)-menthol by recombinant *Candida rugosa* lipase LIP1. *Advanced Synthesis Catalysis*, **344**, 1152–5.

16 Nishizawa, K., Ohgami, Y., Matsuo, N., Kisida, H. and Hirohara, H. (1997) Studies on hydrolysis of chiral, achiral and racemic alcohol esters with *Pseudomonas cepacia* lipase: mechanism of stereospecificity of the enzyme. *Journal of the Chemical Society, Perkin Transactions*, **2**, 1293–8.

17 Tuomi, W.V. and Kazlauskas, R.J. (1999) Molecular basis for enantioselectivity of lipase from *Pseudomonas cepacia* toward primary alcohols. Modeling, kinetics, and chemical modification of Tyr29 to increase or decrease enantioselectivity. *Journal of Organic Chemistry*, **64**, 2638–47.

18 Kwon, D.Y., Hong, Y.-J. and Yoon, S.H. (2000) Enantiomeric synthesis of (*S*)-2-methylbutanoic acid methyl ester, apple flavor, using lipases in organic solvent. *Journal of Agricultural and Food Chemistry*, **48**, 524–30.

19 Ueji, S.-I., Watanabe, K., Koshiba, T., Nakamura, M., Oh-Ishi, K., Yasufuku, Y. and Miyazawa, T. (1999) Lipase-catalyzed esterification of 2-(4-substituted phenoxy)propionic acids in organic solvents: substituent effect controlling enantioselectivity toward racemic acids. *Biotechnology Letters*, **21**, 865–8.

20 Weissfloch, A.N.E. and Kazlauskas, R.J. (2001) Choosing hydrolases for enantioselective reactions involving alcohols using empirical rules, in *Methods in Biotechnology, Vol. 15: Enzymes in Nonaqueous Solvents: Methods and Protocols* (eds E.N. Vulfson, P.J. Halling and H.L. Holland), Humana Press, Totowa, NJ, pp. 243–59.

21 Kazlauskas, R.J., Weissfloch, A.N.E., Rappaport, A.T. and Cuccia, L.A. (1991) A rule to predict which enantiomer of a secondary alcohol reacts faster in reactions catalyzed by cholesterol esterase, lipase from *Pseudomonas cepacia*, and lipase from *Candida rugosa*. *Journal of Organic Chemistry*, **56**, 2656–65.

22 Burgess, K. and Jennings, L.D. (1991) Enantioselective esterifications of unsaturated alcohols mediated by a lipase prepared from *Pseudomonas*. sp. *Journal of the American Chemical Society*, **113**, 6129–39.

23 Naemura, K., Ida, H. and Fukuda, R. (1993) Lipase YS-catalyzed enantioselective transesterification of alcohols of bicarbocyclic compounds. *Bulletin of the Chemical Society of Japan*, **66**, 573–7.

24 Kim, M.J. and Cho, H. (1992) *Pseudomonas* lipases as catalysts in organic synthesis: specificity of lipoprotein lipase. *Journal of the Chemical Society, Chemical Communications*, 1411–13.

25 Roberts, S.M. (1989) Use of enzymes as catalysts to promote key transformations in organic synthesis. *Philosophical Transactions of the Royal Society of London. Series B*, **324**, 577–87.

26 Janssen, A.J.M., Klunder, A.J.H. and Zwanenburg, B. (1991) Resolution of secondary alcohols by enzyme-catalyzed transesterification in alkyl carboxylates as the solvent. *Tetrahedron*, **47**, 7645–62.

27 Kazlauskas, R.J., Weissfloch, A.N.E. (1997) A structure-based rationalization of the enantiopreference of subtilisin toward secondary alcohols and isosteric primary amines (Review). *Journal of Molecular Catalysis B Enzymatic*, **3**, 65–72.

28 Zhang, M. and Kazlauskas, R. (1999) First preparation of enantiopure indane monomer, (*S*)-(−)- and (R)-(+)-2,3-dihydro-3-(4′-hydroxyphenyl)-1,1,3-trimethyl-1*H*-inden-5-ol, via a unique enantio- and regioselective enzymatic kinetic resolution. *Journal of Organic Chemistry*, **64**, 7498–503.

29 Sundaramoorthy, M., Terner, J. and Poulos, T.L. (1998) Stereochemistry of the chloroperoxidase active site: crystallographic and molecular-modeling studies. *Chemistry and Biology*, **5**, 461–73.

30 Holmquist, M., Hæffner, F., Norin, T. and Hult, K. (1996) A structural basis for enantioselective inhibition of *Candida rugosa* lipase by long-chain aliphatic alcohols. *Protein Science*, **5**, 83–8.

31 Botta, M., Cernia, E., Corelli, F., Manetti, F. and Soro, S. (1997) Probing the substrate specificity for lipases. II. Kinetic and modeling studies on the molecular recognition of 2-arylpropionic esters by *Candida rugosa* and *Rhizomucor miehei* lipases. *Biochimica et Biophysica Acta*, **1337**, 302–10.

32 Berglund, P., Holmquist, M. and Hult, K. (1998) Reversed enantiopreference of

Candida rugosa lipase supports different modes of binding enantiomers of a chiral acyl donor. *Journal of Molecular Catalysis B Enzymatic*, **5**, 283–7.

33 Bocola, M., Otte, N., Jaeger, K.-E., Reetz, M.T. and Thiel, W. (2004) Learning from directed evolution: theoretical investigations into cooperative mutations in lipase enantioselectivity. *Chembiochem: A European Journal of Chemical Biology*, **5**, 214–23.

34 Reetz, M.T., Puls, M., Carballeira, J.D., Vogel, A., Jaeger, K.-E., Eggert, T., Thiel, W., Bocola, M. and Otte, N. (2007) Learning from directed evolution: further lessons from theoretical investigations into cooperative mutations in lipase enantioselectivity. *Chembiochem: A European Journal of Chemical Biology*, **8**, 106–12.

35 Schulz, T., Pleiss, J. and Schmid, R.D. (2000) Enantioselectivity of *Pseudomonas cepacia* lipase toward secondary alcohols: a quantitative model. *Protein Science*, **9**, 1053–62.

36 Phillips, R.S. (1992) Temperature effects on stereochemistry of enzymatic reactions. *Enzyme and Microbial Technology*, **14**, 417–19.

37 Overbeeke, P.L.A., Orrenius, S.C., Jongejan, J.A. and Duine, J.A. (1998) Enthalpic and entropic contributions to lipase enantioselectivity. *Chemistry and Physics of Lipids*, **93**, 81–93.

38 Overbeeke, P.L.A., Ottosson, J., Hult, K., Jongejan, J.A. and Duine, J.A. (1999) The temperature dependence of enzymatic kinetic resolutions reveals the relative contribution of enthalpy and entropy to enzymatic enantioselectivity. *Biocatalysis and Biotransformation*, **17**, 61–79.

39 Ottosson, J., Rotticci-Mulder, J.C., Rotticci, D. and Hult, K. (2001) Rational design of enantioselective enzymes requires considerations of entropy. *Protein Science*, **10**, 1769–74.

40 Ottosson, J., Fransson, L. and Hult, K. (2002) Substrate entropy in enzyme enantioselectivity: an experimental and molecular modeling study of a lipase. *Protein Science*, **11**, 1462–71.

41 Helms, V. and Wade, R.C. (1998) Computational alchemy to calculate absolute protein-ligand binding free energy. *Journal of the American Chemical Society*, **120**, 2710–13.

42 Massova, I. and Kollman, P.A. (1999) Computational alanine scanning to probe protein-protein interactions: a novel approach to evaluate binding free energies. *Journal of the American Chemical Society*, **121**, 8133–43.

43 Stanton, R.V., Perakyla, M., Bakowies, D. and Kollman, P.A. (1998) Combined ab initio and free energy calculations to study reactions in enzymes and solution–amide hydrolysis in trypsin and aqueous solution. *Journal of the American Chemical Society*, **120**, 3448–57.

44 Ke, T. and Klibanov, A.M. (1998) Insights into the solvent dependence of chymotryptic prochiral selectivity. *Journal of the American Chemical Society*, **120**, 4259–63.

45 Colombo, G., Ottolina, G., Carrea, G., Bernardi, A. and Scolastico, C. (1998) Application of structure-based thermodynamic calculations to the rationalization of the enantioselectivity of subtilisin in organic solvents. *Tetrahedron: Asymmetry*, **9**, 1205–14.

46 Savile, C.K. and Kazlauskas, R.J. (2005) How substrate solvation contributes to the enantioselectivity of subtilisin toward secondary alcohols. *Journal of the American Chemical Society*, **127**, 12228–9.

47 Leonard, V., Fransson, L., Lamare, S., Hult, K. and Graber, M. (2007) A water molecule in the stereospecificity pocket of *Candida antarctica* lipase B enhances enantioselectivity towards pentan-2-ol. *Chembiochem: A European Journal of Chemical Biology*, **8**, 662–7.

48 Ottosson, J., Fransson, L., King, J.W. and Hult, K. (2002) Size as a parameter for solvent effects on *Candida antarctica* lipase B enantioselectivity. *Biochimica et Biophysica Acta*, **1594**, 325–34.

49 Tantillo, D.J. and Houk, K.N. (1999) Fidelity in hapten design: how analogous are phosphonate haptens to the transition states for alkaline hydrolysis of aryl esters. *Journal of Organic Chemistry*, **64**, 3066–76.

50 Colombo, G., Toba, S. and Merz, K.M. Jr (1999) Rationalization of the enantioselectivity of subtilisin in DMF. *Journal of the American Chemical Society*, **121**, 3486–93.

51 (a) Truhlar, D.G., Gao, J., Alhambra, C., Garcia-Viloca, M., Corchado, J., Sánchez, M.L. and Villà, J. (2002) The incorporation of quantum effects in enzyme kinetics modeling. *Accounts of Chemical Research*, **35**, 341–9.
(b) Pu, J., Gao, J. and Truhlar, D.G. (2006) Multidimensional tunneling, recrossing, and the transmission coefficient for enzymatic reactions. *Chemical Reviews*, **106**, 3140–69.

52 Zuegg, J., Hönig, H., Schrag, J.D. and Cygler, M. (1997) Selectivity of lipases: conformational analysis of suggested intermediates in ester hydrolysis of chiral primary and secondary alcohols. *Journal of Molecular Catalysis B Enzymatic*, **3**, 83–98.

53 Orrenius, C., Hæffner, F., Rotticci, D., Ohrner, N., Norin, T. and Hult, K. (1998) Chiral recognition of alcohol enantiomers in acyl transfer reactions catalysed by *Candida antarctica* lipase B. *Biocatalysis and Biotransformation*, **16**, 1–15.

54 Rotticci, D., Hæffner, F., Orrenius, C., Norin, T. and Hult, K. (1998) Molecular recognition of *sec*-alcohol enantiomers by *Candida antarctica* lipase B. *Journal of Molecular Catalysis B Enzymatic*, **5**, 267–72.

55 Nakamura, K., Kawasaki, M. and Ohno, A. (1994) Effects of substrate structure on lipase-catalyzed transesterification of ω-substituted 1-alkanols in organic solvents. *Bulletin of the Chemical Society of Japan*, **67**, 3053–6.

56 Nakamura, K., Kawasaki, M. and Ohno, A. (1996) Lipase-catalyzed transesterification of aryl-substituted alkanols in an organic solvent. *Bulletin of the Chemical Society of Japan*, **69**, 1079–85.

57 Haeffner, F., Norin, T. and Hult, K. (1998) Molecular modeling of the enantioselectivity in lipase-catalyzed transesterification reactions. *Biophysical Journal*, **74**, 1251–62.

58 Pineda, J.R.E.T. and Schwartz, S.D. (2006) Protein dynamics and catalysis: the problems of transition state theory and the subtlety of dynamic control. *Philosophical Transactions of the Royal Society of London. Series B, Biological Sciences*, **361**, 1433–8.

59 Olsson, M.H.M., Mavri, J. and Warshel, A. (2006) Transition state theory can be used in studies of enzyme catalysis: lessons from simulations of tunnelling and dynamical effects in lipoxygenase and other systems. *Philosophical Transactions of the Royal Society of London. Series B Biological Sciences*, **361**, 1417–32.

60 Guieysse, D., Salagnad, C., Monsan, P., Remaud-Simeon, M. and Tran, V. (2003) Towards a novel explanation of *Pseudomonas cepacia* lipase enantioselectivity via molecular modelling of the enantiomer trajectory into the active site. *Tetrahedron: Asymmetry*, **14**, 1807–17.

61 Ozaki, S.-I. and de Montellano, P.R. (1994) Molecular engineering of horseradish peroxidase. Highly enantioselective sulfoxidation of aryl alkyl sulfides by the Phe-41→Leu mutant. *Journal of the American Chemical Society*, **116**, 4487–8.

62 Savenkova, M.I., Newmyer, S.L. and de Montellano, P.R. (1996) Rescue of His-42 Ala horseradish peroxidase by a Phe-41 His mutation. Engineering of a surrogate catalytic histidine. *The Journal of Biological Chemistry*, **271**, 24598–603.

63 van Loo, B., Lutje Spelberg, J.H., Kingma, J., Sonke, T., Wubbolts, M.G. and Janssen, D.B. (2004) Directed evolution of epoxide hydrolase from *A. radiobacter* toward higher enantioselectivity by error-prone PCR ad DNA shuffling. *Chemistry and Biology*, **11**, 981–90.

64 Magnusson, A., Hult, K. and Holmquist, M. (2001) Creation of an enantioselective hydrolase by engineered substrate-assisted catalysis. *Journal of the American Chemical Society*, **123**, 4354–5.

65 Reetz, M.T., Wilensek, S., Zha, D. and Jaeger, K.-E. (2001) Directed evolution of an enantioselective enzyme through combinatorial multiple-cassette mutagenesis. *Angewandte Chemie – International Edition*, **40**, 3589–91.

66 Park, S., Morley, K.L., Horsman, G.P., Holmquist, M., Hult, K. and Kazlauskas, R.J. (2005) Focusing mutations into the substrate-binding site of *Pseudomonas fluorescens* esterase increases the enantioselectivity more effectively than

random mutagenesis. *Chemistry and Biology*, **11**, 45–54.

67 Henke, E., Bornscheuer, U.T., Schmid, R.D. and Pleiss, J. (2003) A molecular mechanism of enantiorecognition of tertiary alcohols by carboxylesterases. *Chembiochem: A European Journal of Chemical Biology*, **4**, 485–93.

68 Ema, T., Fujii, T., Ozaki, M., Korenaga, T. and Sakai, T. (2005) Rational control of enantioselectivity of lipase by site-directed mutagenesis based on the mechanism. *Chemical Communications*, 4650–1.

69 Rink, R., Lutje-Spelberg, J.H., Pieters, R.J., Kingma, J., Nardini, M., Kellogg, R.M., Dijkstra, B.W. and Janssen, D.B. (1999) Mutation of tyrosine residues involved in the alkylation half reaction of epoxide hydrolase from *Agrobacterium radiobacter* AD1 results in improved enantioselectivity. *Journal of the American Chemical Society*, **121**, 7417–18.

70 Tang, L., van Merode, A.E.J., Lutje Spelberg, J.H., Fraaije, M.W. and Janssen, D.B. (2003) Steady-state kinetics and tryptophan fluorescence properties of halohydrin dehalogenase from *Agrobacterium radiobacter*. Roles of W139 and W249 in the active site and halide-induced conformational change. *Biochemistry*, **42**, 14057–65.

71 Scheib, H., Pleiss, J., Stadler, P., Kovac, A., Potthoff, A.P., Haalck, L., Spener, F., Paltauf, F. and Schmid, R.D. (1998) Rational design of *Rhizopus oryzae* lipase with modified stereoselectivity toward triradylglycerols. *Protein Engineering*, **11**, 675–82.

72 van Herk, T., Hartog, A.F., Ruijssenaars, H.J., Kerkman, R., Schoemaker, H.E. and Wever, R. (2007) Optimization of the kinetic resolution of the DL-phosphomonoesters of threonine and serine by random mutagenesis of the acid phosphatase from *Salmonella enterica*. *Advanced Synthesis Catalysis*, **349**, 1349–52.

73 Carboni, C., Kierkels, H.G.T., Gardossi, L., Tamiola, K., Janssen, D.B. and Quaedflieg, P.J.L.M. (2006) Preparation of D-amino acids by enzymatic kinetic resolution using a mutant of penicillin-G acylase from *E. coli*. *Tetrahedron: Asymmetry*, **17**, 245–51.

74 Rotticci, D., Rotticci-Mulder, J.C., Denman, S., Norin, T. and Hult, K. (2001) Improved enantioselectivity of a lipase by rational protein engineering. *Chembiochem: A European Journal of Chemical Biology*, **2**, 766–70.

75 May, O., Nguyen, P.T. and Arnold, F.H. (2000) Inverting enantioselectivity by directed evolution of hydantoinase for improved production of L-methionine. *Nature Biotechnology*, **18**, 317–20.

76 Chen-Goodspeed, M., Sogorb, M.A., Wu, F. and Raushel, F.M. (2001) Structural determinants of the substrate and stereochemical specificity of phosphotriesterase. *Biochemistry*, **40**, 1325–31.

77 Chen-Goodspeed, M., Sogorb, M.A., Wu, F. and Raushel, F.M. (2001) Enhancement, relaxation, and reversal of the stereoselectivity for phosphotriesterase by rational evolution of active site residues. *Biochemistry*, **40**, 1332–9.

78 Rui, L., Cao, L., Chen, W., Reardon, K.F. and Wood, T.K. (2005) Protein engineering of epoxide hydrolase from *Agrobacterium radiobacter* AD1 for enhanced activity and enantioselective production of (*R*)-1-phenylethane-1,2-diol. *Applied and Environmental Microbiology*, **71**, 3995–4003.

79 Lingen, B., Grötzinger, J., Kolter, D., Kula, M.-R. and Pohl, M. (2002) Improving the carboligase activity of benzoylformate decarboxylase from *Pseudomonas putida* by a combination of directed evolution and site-directed mutagenesis. *Protein Engineering*, **15**, 585–93.

80 Kotik, M., Stepanek, V., Kyslik, P. and Maresova, H. (2007) Cloning of an epoxide hydrolase-encoding gene from *Aspergillus niger* M200, overexpression in *E. coli*, and modification of activity and enantioselectivity of the enzyme by protein engineering. *Journal of Biotechnology*, **132**, 8–15.

81 Manco, G., Carrea, G., Giosue, E., Ottolina, G., Adamo, G. and Rossi, M. (2002) Modification of the enantioselectivity of two homologous thermophilic carboxylesterases from *Alicyclobacillus acidocaldarius* and *Archaeoglobus fulgidus* by random

mutagenesis and screening. *Extremophiles*, **6**, 325–31.

82 Holmquist, M., Martinelle, M., Berglund, P., Clausen, I.G., Patkar, S., Svendsen, A. and Hult, K. (1993) Lipases from *Rhizomucor miehei* and *Humicola lanuginosa*: modification of the lid covering the active site alters enantioselectivity. *Journal of Protein Chemistry*, **12**, 749–57.

83 Horsman, G.P., Liu, A.M.F., Henke, E., Bornscheuer, U.T. and Kazlauskas, R.J. (2003) Mutations in distant residues moderately increase the enantioselectivity of *Pseudomonas fluorescens* esterase toward methyl 3-bromo-2-methylpropanonate and ethyl 3-phenylbutyrate. *Chemistry – A European Journal*, **9**, 1933–9.

84 Morley, K.L. and Kazlauskas, R.J. (2005) Improving enzyme properties: when are closer mutations better? *Trends in Biotechnology*, **23**, 231–7.

85 Schwede, T., Kopp, J., Guex, N. and Peitsch, M.C. (2003) SWISS-MODEL: an automated protein homology-modeling server. *Nucleic Acids Research*, **31**, 3381–5.

86 Clayden, J., Lund, A., Vallverdú, L. and Helliwell, M. (2004) Ultra-remote stereocontrol by conformational communication of information along a carbon chain. *Nature*, **431**, 966–71.

87 Lipkowitz, K.B., D'Hue, C.A., Sakamoto, T. and Stack, J.N. (2002) Stereocartography: a computational mapping technique that can locate regions of maximum stereoinduction around chiral catalysts. *Journal of the American Chemical Society*, **124**, 14255–67.

88 Parales, R.E., Resnick, S.M., Yu, C.-L., Boyd, D.R., Sharma, N.D. and Gibson, D.T. (2000) Regioselectivity and enantioselectivity of naphthalene dioxygenase during arene *cis* -dihydroxylation: control by phenylalanine 352 in the a subunit. *Journal of Bacteriology*, **182**, 5495–504.

89 Hirose, Y., Kariya, K., Nakanishi, Y., Kurono, Y. and Achiwa, K. (1995) Inversion of enantioselectivity in hydrolysis of 1,4-dihydropyridines by point mutation of lipase PS. *Tetrahedron Letters*, **36**, 1063–6.

90 Koga, Y., Kato, K., Nakano, H. and Yamane, T. (2003) Inverting enantioselectivity of *Burkholderia cepacia* KWI-56 lipase by combinatorial mutagenesis and high-throughput screening using single molecule PCR and in vitro expression. *Journal of Molecular Biology*, **331**, 585–92.

91 Ivancic, M., Valinger, G., Gruber, K. and Schwab, H. (2007) Inverting enantioselectivity of *Burkholderia gladioli* esterase EstB by directed and designed evolution. *Journal of Biotechnology*, **129**, 109–22.

92 Bartsch, S., Kourist, R. and Bornscheuer, U.T. (2008) Complete inversion of enantioselectivity towards acetylated tertiary alcohols by a double mutant of a *Bacillus subtilis* esterase. *Angewandte Chemie – International Edition*, **47**, 1508–11.

93 Zha, D., Wilensek, S., Hermes, M., Jaeger, K.-E. and Reetz, M.T. (2001) Complete reversal of enantioselectivity of an enzyme-catalyzed reaction by directed evolution. *Chemical Communications*, 2664–5.

94 Magnusson, A.O., Takwa, M., Hamberg, A. and Hult, K. (2005) An *S*-selective lipase was created by rational redesign and the enantioselectivity increased with temperature. *Angewandte Chemie – International Edition*, **44**, 4582–5.

95 van den Heuvel, R.H.H., Fraaije, M.W., Ferrer, M., Mattevi, A. and van Berkel, W. J.H. (2000) Inversion of stereospecificity of vanillyl-alcohol oxidase. *Proceedings of the National Academy of Sciences of the United States of America*, **97**, 9455–60.

96 Terao, Y., Ijima, Y., Miyamoto, K. and Ohta, H. (2007) Inversion of enantioselectivity of arylmalonate decarboxylase via site-directed mutation based on the proposed reaction mechanism. *Journal of Molecular Catalysis B Enzymatic*, **45**, 15–20.

97 Li, Y., Aubert, S.D., Maes, E.G. and Raushel, F.M. (2004) Enzymatic resolution of chiral phosphinate esters. *Journal of the American Chemical Society*, **126**, 8888–9.

keywords/abstract

Dear author,
Please check and/or supply keywords (3 to 5) and an abstract. These will not be included in the print version of your chapter but in the online version. If you do not supply an abstract, the section heading will be used instead.
Thank you!

Abstract

Enantioselective enzyme reactions are enzyme-catalyzed reactions that discriminate between enantiomeric substrates or products. Enzymes are enantioselective because they stabilize the transition state for fast-reacting enantiomer more effectively than for the slow-reacting enantiomer. Orienting the fast-reacting enantiomer in the active site is usually straightforward, but the slow-reacting enantiomer orientation is more difficult to predict because several orientations are possible. Some orientations involve exchanged locations of two substituents; other orientations involve an umbrella-like inversion where only one substituent (usually hydrogen) lies in a new location. High enantioselectivity requires the destabilization of all possible orientations for the slow-reacting enantiomer and different orientations require different strategies for destabilization. Protein engineering using rational design or random mutagenesis shows that mutations closer to the active site increase enantioselectivity more effectively than those far from the active site. Protein engineering can also reverse enantioselectivity by moving binding sites or key catalytic residues.

Keywords

enantioselectivity; lipases; kinetic resolution; X-ray crystal structure; computer modeling; random mutagenesis; site-directed mutagenesis; reversing enantioselectivity.

AUTHOR QUERIES

Dear Author,

During the preparation of your manuscript for publication, the questions listed below have arisen. Please attend to these matters and return this form with your proof.

Many thanks for your assitstance.

Query References	Query	Remarks
1	Author: Please update the page range.	

C